Articles

Photolabeling of the Phosphate Binding Site of Mitochondrial F_1-ATPase by [^{32}P]Azidonitrophenyl Phosphate. Identification of the Photolabeled Amino Acid Residues†

Jérôme Garin,*,‡ Laurent Michel,‡ Alain Dupuis,‡ Jean-Paul Issartel,‡ Joël Lunardi,‡ Jürgen Hoppe,§ and Pierre Vignais‡

Laboratoire de Biochimie, Département de Recherche Fondamentale, Centre d'Etudes Nucléaires, 85X, 38041 Grenoble Cedex, France, and Institut für Physiologische Chemie, Universität Würzburg, Koellickerstrasse 2, D-8700 Wurzburg, FRG

Received August 1, 1988; Revised Manuscript Received October 3, 1988

ABSTRACT: [^{32}P]Azidonitrophenyl phosphate ([^{32}P]ANPP) is a photoactivatable analogue of P_i. It competes efficiently with P_i for binding to the F_1 sector of beef heart mitochondrial ATPase and photolabels the P_i binding site located in the β subunit of F_1 [Lauquin, G. J. M., Pougeois, R., & Vignais, P. V. (1980) *Biochemistry 19*, 4620-4626]. By cleavage of the photolabeled β subunit of F_1 with cyanogen bromide, trypsin, and chymotrypsin, bound [^{32}P]ANPP was localized in a fragment spanning Thr 299-Phe 326. By Edman degradation of the radiolabeled tryptic peptide spanning Ile 296-Arg 337, [^{32}P]ANPP was found to be attached covalently by its photoreactive group to Ile 304, Gln 308, and Tyr 311. These results are discussed in terms of a model in which the phosphate group of [^{32}P]ANPP interacts with a glycine-rich sequence of the β subunit, spanning Gly 156-Lys 162, which is spatially close to the photolabeled Ile 304-Tyr 311 segment of the same subunit.

The mapping of the binding sites for the substrates of F_1-ATPases,[1] namely, ATP, ADP, and P_i, is central to our understanding of the mechanism of ATP hydrolysis or synthesis by this enzyme. Whereas the nucleotide binding sites of F_1-ATPases have been extensively studied, little is known about the topography of their respective phosphate binding sites. Penefsky (1977) first described the specific, reversible interaction of mitochondrial F_1 with P_i. He also showed that agents which influenced F_1-ATPase activity also influenced P_i binding; for example, P_i binding was inhibited by ADP and ATP, and more efficiently by AMPP(NH)P, a slowly hydrolyzable ATP analogue (Tomaszek & Schuster, 1986) which binds to F_1 with high affinity. This suggested the possibility that the P_i binding site in F_1 is shared by the γ-phosphate group of ATP.

At present, two analogues of P_i, namely, potassium ferrate and 2-azido-4-nitrophenyl phosphate (ANPP), have been used in mapping studies. The ferrate anion has been shown to oxidize amino acid residues likely to be located in or near the binding sites for P_i or phosphorylated substrates in phosphorylase *b* (Lee & Benisek, 1978), triosephosphate isomerase (Steczko et al., 1983), and adenylate kinase (Crivellone et al., 1985). ANPP is another useful probe which competes with P_i for binding to mitochondrial F_1 in the dark, with a K_i value of 60 μM (Lauquin et al., 1980). ANPP also binds to *Escherichia coli* F_1 (Pougeois et al., 1983a) and chloroplast F_1 (Pougeois et al., 1983b), and it has been used to photolabel not only H^+-ATPases but also the mitochondrial P_i carrier (Lauquin et al., 1980; Tommasino et al., 1987). The goal of this work was to identify the amino acid residues of the β subunit which are labeled after photoirradiation of mitochondrial F_1 with [^{32}P]ANPP.

Materials and Methods

Chemicals. The sources of the chemicals were as follows: trypsin, Worthington; α-chymotrypsin, Miles; PITC and DITC glass beads, Pierce Chemicals; silica gel 60F254 aluminum plates, Merck; $H_3{}^{32}PO_4$ (10 mCi), New England Nuclear; 4-amino-2-nitrophenol, Aldrich. All reagents used were of the purest grade commercially available.

Synthesis of 4-Azido-2-nitrophenol. 4-Azido-2-nitrophenol (ANP) was synthesized from 4-amino-2-nitrophenol as described by Lauquin et al. (1980). The purity of 4-azido-2-nitrophenol was checked by thin-layer chromatography on silica gel plates (silica gel 60F254) in NH_4OH/dioxane/2-propanol/H_2O (6/5/3.5/1 v/v). A single yellow spot with an R_f of 0.92 was observed. The identity of the product was verified by ^{13}C NMR and mass spectrometry.

Synthesis of [^{32}P]-4-Azido-2-nitrophenyl Phosphate ([^{32}P]ANPP). The synthesis of [^{32}P]ANPP was first reported by Lauquin et al. (1980). The original method was modified with the aim of shortening the time of synthesis. ANP was phosphorylated by the method of Symons (1968). A solution of 10 mCi of [^{32}P]P_i, diluted with 12 μmol of unlabeled P_i, was added to 65 mg of ANP in acetonitrile. After evaporation to dryness, the residue was solubilized with 1 mL of anhydrous

† This work was supported by grants from the Centre National de la Recherche Scientifique (CNRS/UA 1130) and the Faculté de Médecine, Université Joseph Fourier de Grenoble.

* Address correspondence to this author at DRF/Biochimie, C.E. N.-G., 85X, 38041 Grenoble Cedex, France.

‡ Centre d'Etudes Nucléaires.

§ Universität Würzburg.

[1] Abbreviations: ANPP, 4-azido-2-nitrophenyl phosphate; AMPP(NH)P, 5'-adenylyl imidodiphosphate; PITC, phenyl isothiocyanate; DITC, phenylene diisothiocyanate; DMSO, dimethyl sulfoxide; FSBI, 5'-[*p*-(fluorosulfonyl)benzoyl]inosine; F_1, catalytic sector (soluble) of the ATPase complex; TDAB, tetradecyltrimethylammonium bromide; TFA, trifluoroacetic acid; AMEDA, P^1-(5'-adenosyl) P^2-*N*-(2-mercaptoethyl)diphosphoramidate.

0006-2960/89/0428-1442$01.50/0 © 1989 American Chemical Society

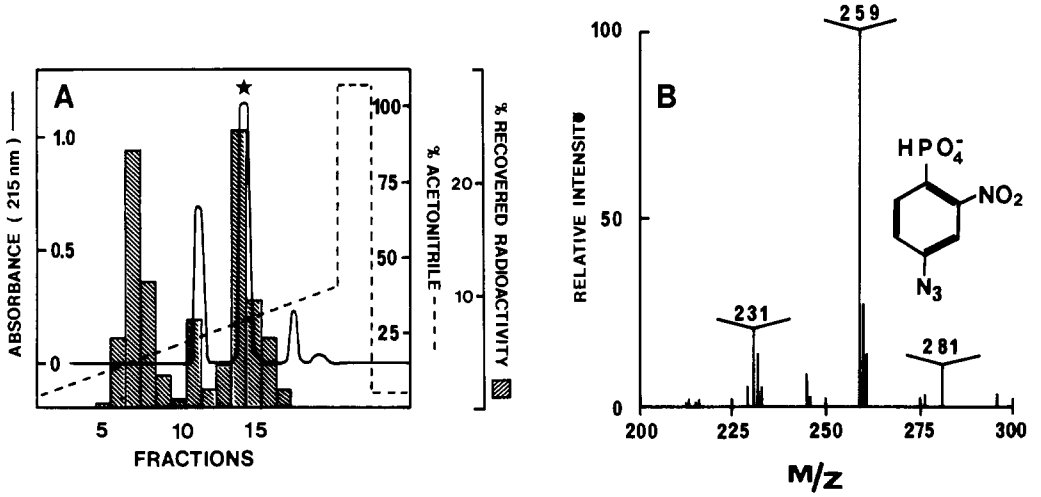

FIGURE 1: Panel A: Purification of [^{32}P]ANPP by HPLC. The column (Waters, C_{18} preparative) was equilibrated in 95% buffer A (0.1% TFA) and 5% buffer B (0.1% TFA, 99.9% acetonitrile). The aqueous solution (500 μL) containing [^{32}P]ANPP (see Materials and Methods) was injected in the column, and a gradient of acetonitrile was applied at a flow rate of 2 mL·min^{-1}. Fractions were collected at 1-min intervals. The [^{32}P]ANPP peak is indicated by a star. Panel B: Fast atom bombardment mass spectrum of purified ANPP, showing the corresponding ion at m/z 259. Insert: Structure of 4-azido-2-nitrophenyl phosphate (ANPP).

acetonitrile previously distilled and stored on calcium hydride. Acetonitrile was removed by evaporation. This cycle of solubilization by acetonitrile and evaporation was repeated twice. To the dry residue, 400 μL of dimethyl sulfoxide was added, followed by 32 μL of triethylamine and 28 μL of trichloroacetonitrile, and the mixture was stirred for 30 min at 37 °C. The water-soluble [^{32}P]ANPP was extracted repeatedly by 2 mL of water; after four successive extractions, 95% of the radioactivity was recovered in the aqueous phase. The water-insoluble ANP, present as contaminant of [^{32}P]ANPP, was removed by two successive extractions with 5 mL of diethyl ether. The aqueous phase containing [^{32}P]ANPP was evaporated to dryness. The residue, solubilized in 500 μL of distilled water, was purified by HPLC using a C_{18} μBondapak preparative column (Waters). Usually, separation of phosphorylated molecules by reverse-phase HPLC (Anderson & Murphy, 1976; Hartwick et al., 1978) or anion-exchange HPLC (Mac Keag & Brown, 1978) involves solvents containing inorganic phosphate; obviously these methods were inappropriate to purify ANPP, as the phosphate present in the eluting buffer would later compete with ANPP in binding studies. We therefore developed a reverse-phase HPLC separation using phosphate-free solvents, namely, TFA, water, and acetonitrile. Unreacted [^{32}P]P_i was eluted in fractions 6–9, whereas [^{32}P]ANPP was recovered in fractions 14–16 (Figure 1A). The purity of [^{32}P]ANPP was checked by thin-layer chromatography on silica plates by using the same phase as that previously described. A single radioactive and UV- absorbing spot, with an R_f of 0.58, was revealed. On the basis of UV absorbance and radioactivity measurement, the yield of [^{32}P]ANPP recovered was estimated to be about 40% with respect to the added [^{32}P]P_i; this high yield allowed the synthesis of the photoprobe with very high specific activity (up to 2000 dpm/pmol). The identity of the purified product was ascertained by fast atom bombardment mass spectrometry. The spectrum (Figure 1B) revealed the presence of the anion $ANPP^-$ at m/z 259, fragments that corresponded to elimination of nitrogen at m/z 231, and accumulation of hydrogenation products at m/z 232 and 233. The peak at m/z 281 corresponded to the monosodium salt of ANPP (Na^+ $ANPP^{2-}$).

Preparation of Bovine Mitochondrial F_1. Beef heart mitochondria were prepared as described by Smith (1967). Beef heart mitochondrial F_1 was prepared according to the method of Knowles and Penefsky (1972) modified by Klein et al. (1982). It was stored as an ammonium sulfate precipitate at 4 °C in a medium consisting of 50 mM Tris-HCl, 250 mM sucrose, 2 mM EDTA, 4 mM ATP, and 2.1 M $(NH_4)_2SO_4$, final pH 8.0.

Photoaffinity Labeling of F_1 with [^{32}P]ANPP. Purification and Fragmentation of the Photolabeled β Subunit. The F_1 suspension in ammonium sulfate was centrifuged, and the pellet was solubilized in 250 mM sucrose and 50 mM Tris–acetate, final pH 7.5 (medium A). The F_1 solution was desalted with an AcA 202 column (IBF) equilibrated with medium A, and then passed through another AcA 202 column equilibrated with 50 mM MES–Tris and 1 mM $MgSO_4$, final pH 7.5 (medium B). The F_1 preparation adjusted to 10 μM was incubated for 20 min in darkness with 50 μM [^{32}P]ANPP in a small Petri dish and then subjected to four successive photoirradiations for 30 s each time, using a Xenon XB 100 lamp (1000 W) equipped with a parabolic reflector and placed at 10 cm from the F_1 preparation. A glass plate was placed between the light source and the F_1 sample to eliminate short-wavelength UV light. No loss of enzymatic activity of native F_1 photoirradiated in the absence of ANPP was detected. The photolabeled F_1 was precipitated by ammonium sulfate (65%) and sedimented by centrifugation. Most of the unbound [^{32}P]ANPP was removed with the supernatant. Photolabeled F_1 was solubilized and dissociated into subunits, using a medium consisting of 50 mM sodium succinate, 1 M sodium chloride, 0.25 M sodium nitrate, 0.1 mM dithiothreitol, and 4 mM EDTA (Issartel et al., 1983). Residual traces of unbound [^{32}P]ANPP were eliminated by dialysis against the same medium. The photolabeled β subunit was purified by chromatography on DE-52 cellulose (Whatman) with a linear LiCl gradient (Issartel et al., 1983). It was succinylated (Lunardi et al., 1987) and then fragmented by cyanogen bromide and trypsin or α-chymotrypsin. The method used was essentially similar to that adopted for exploring the region of the β subunit photolabeled by [^{32}P]-2-azido ADP (Garin et al., 1986). The resulting peptides were fractionated by gel filtration at 4 °C or by reverse-phase HPLC using either a C_{18} μBondapak column (Waters) or a C_8 Aquapore column (Brownlee). The nomenclature of peptides resulting from chemical or enzymatic cleavage of the β subunit was that

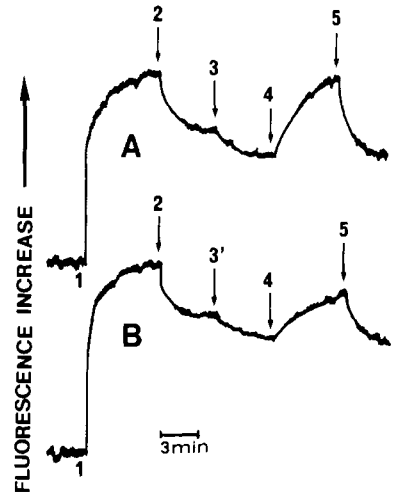

FIGURE 2: Compared effects of P_i and ANPP on the fluorescence intensity of aurovertin–F_1 complex. Assays were carried out at 30 °C. F_1 (0.18 μM) was incubated with 0.5 μM aurovertin in 2 mL of a medium containing 0.15 M sucrose, 50 mM Tris-HCl, pH 7.5, and 30 mM NaCl. Arrows correspond to the following additions: (1) aurovertin D; (2) 5 mM $MgCl_2$; (3) 0.65 mM NaP_i; (3′) 0.18 mM ANPP; (4) 0.1 mM ADP; (5) 1 mM ATP.

adopted by Runswick and Walker (1983); in brief, peptides produced by CNBr cleavage were designated CB peptides, while those arising from trypsin and chymotrypsin cleavage were designated R and Rc peptides.

Amino Acid Analysis and Sequence Analysis. Peptides obtained by fragmentation of the β subunit were hydrolyzed under vacuum in a Waters Pico-Tag work station and derivatized with PITC according to the instructions of the manufacturers. The PTC-amino acid residues were analyzed by chromatography on a Pico-Tag column, and their elution was detected at 254 nm by using a Lambda Max Model 481 (Waters) spectrophotometer.

The amino acid sequence of peptide R_{18} was analyzed by solid-phase Edman degradation. The N-terminal residue of this peptide was reacted with PITC, and the C-terminal arginine (β-Arg 337) was converted to ornithine by hydrazinolysis (Morris et al., 1973). Free hydrazine was removed by chromatography on a P-2 Bio-Gel column (Bio-Rad) equilibrated with 100 mM ammonium hydrogen carbonate. The modified R_{18} peptide was lyophilized and attached to DITC beads as described by Chang (1979). The beads were washed with 0.5 M $NaHCO_3$, water, and methanol sequentially. The yield of binding was about 40%. The peptide was sequenced in a solid-phase sequencer, and the PTH-amino acids were analyzed by using the narrow bore system (2 mm × 22 cm column) designed by Applied Biosystems (Hoppe et al., 1986).

Fluorescent assays with aurovertin D were performed as reported by Issartel et al. (1983) with the following modification: the excitation wavelength was set up at 400 nm to minimize the filter effect due to ANPP, and correction was done as described by Birdsall et al. (1983). The protein concentration was estimated by the Bradford method (1976). Radioactivity was measured by liquid scintillation (Patterson & Greene, 1965). TDAB gel electrophoresis was performed as described by Amory et al. (1980).

RESULTS

Specificity of the [^{32}P]ANPP Binding to Mitochondrial F_1. [^{32}P]ANPP was previously shown to compete with P_i for binding to bovine mitochondrial F_1 and to photolabel selectively the β subunit (Lauquin et al., 1980). In the present work, the

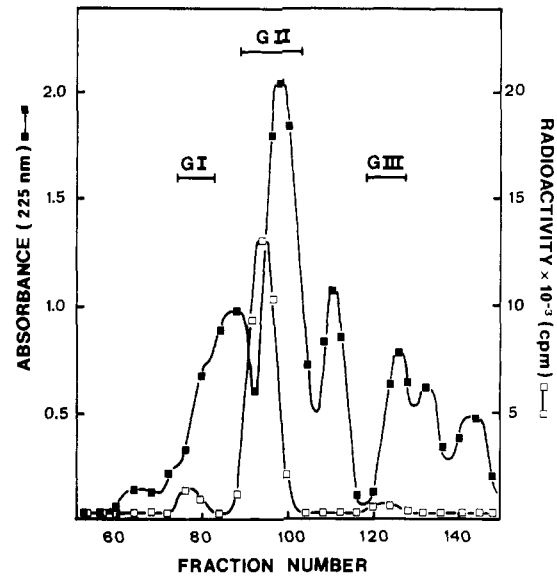

FIGURE 3: Fractionation of CNBr cleavage products of β subunit isolated from mitochondrial F_1 photolabeled with [^{32}P]ANPP. The photolabeled β subunit was isolated from the other subunits of F_1 and cleaved at methionyl residues by CNBr. The CNBr cleavage fragments (see Materials and Methods) were fractionated by chromatography on a Sephadex G-75 superfine column (100 × 2 cm) in 50 mM ammonium bicarbonate. Two-milliliter fractions were collected. Twenty microliters of each fraction was analyzed for its radioactivity content. The bars correspond to the pooled fractions (noted GI, GII, and GIII).

specificity of ANPP for the P_i binding site of F_1 was further evidenced by experiments dealing with modifications of the fluorescence of the F_1–aurovertin D complex upon binding of F_1 substrates: ANPP was shown to mimic P_i by quenching the fluorescence of the aurovertin–F_1 complex, whereas ADP stimulated it (Figure 2). This result provides additional evidence that ANPP behaves as a true P_i analogue with respect to F_1, and not as an ADP analogue as had been suggested earlier (Beharry & Gresser, 1987).

Purification and Identification of Radioactive Fragments in a Digest of β Subunit Photolabeled by [^{32}P]ANPP. Photoirradiation of 100 nmol of mitochondrial F_1 in the presence of [^{32}P]ANPP resulted in covalent binding of about 0.3 mol of photoprobe/mol of F_1. After dissociation of the labeled enzyme into subunits and separation of the subunits by chromatography on DE-52 cellulose (see Materials and Methods), 90% of the radioactivity was recovered in the β subunit peak. The 10% radioactivity found in the $\alpha\gamma\delta\epsilon$ peak was partly due to contaminant β as shown in another study (Issartel et al., 1983). TDAB–polyacrylamide gel electrophoresis of photolabeled F_1 indicated that 95% of the radioactivity was located in the β subunit. The slight photolabeling of the α subunit (about 5%) was not prevented by preincubation with 2 mM P_i, indicating that it was unspecific. On the contrary, photolabeling of the β subunit was prevented by preincubation with P_i.

The photolabeled β subunit (about 190 nmol) was succinylated and submitted to CNBr cleavage. The resulting peptide fragments were fractionated by gel filtration on a Sephadex G-75 column (Figure 3). One major radioactive peak, referred to as GII and containing 87% of the radioactivity, was eluted. It was accompanied by two minor peaks, GI and GIII, containing 9% and 4% of the radioactivity, respectively. The material of peak GIII was not further investigated. Peak GI contained high molecular weight peptides, which arose from incomplete cleavage of the β subunit by CNBr.

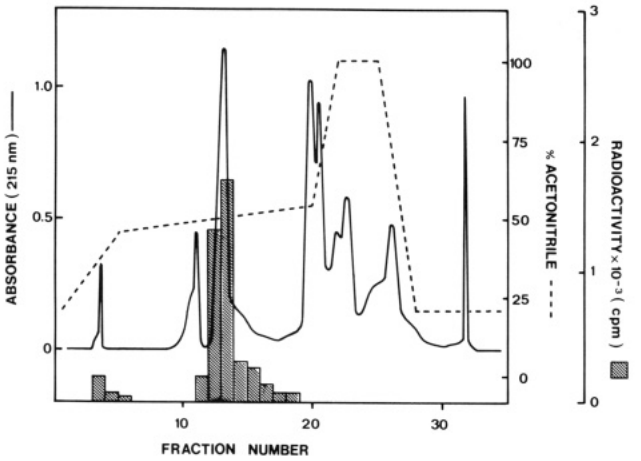

FIGURE 4: Purification of the radioactive CNBr peptide present in the GII fraction by HPLC. The column of C_{18} μBondapak was equilibrated in 80% buffer A (0.1% TFA) and 20% buffer B (0.1% TFA, 99.9% acetonitrile). The material corresponding to the GII fraction (see Figure 3) was injected, and the column was subjected to an acetonitrile gradient at a flow rate of 1 mL·min^{-1}. Ten-microliter aliquots were collected at 1-min intervals and analyzed for the radioactivity content. Ninety percent of the recovered radioactivity was present in fractions 12–18.

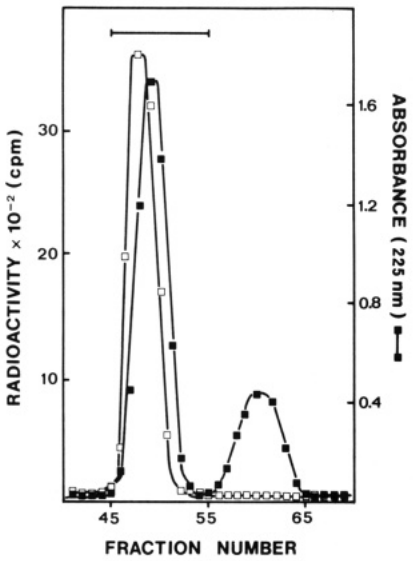

FIGURE 5: Fractionation of a tryptic digest of photolabeled CB9 by gel chromatography. Sixty nanomoles of peptide CB9 was digested by trypsin as described under Materials and Methods. The tryptic digest was applied to a Bio-Gel P-4 column (80 × 1.5 cm) equilibrated with 100 mM ammonium bicarbonate. One and a half milliliter fractions were collected, from which five-microliter fractions were withdrawn for determination of radioactivity.

To identify the radioactive peptide of peak GII, the material of this peak corresponding to fractions 85–105 (Figure 3) was concentrated and subjected to reverse-phase HPLC (Figure 4). Most of the radioactivity was eluted as a single peak whose material, referred to as peptide 1, was analyzed for amino acid composition and N-terminal amino acid identification. Peptide 1 contained the same amino acids and the same N-terminal amino acid, namely, glutamine, as peptide CB9 spanning Gln 293-Met 358.

For a better resolution of the photolabeled portion of the β subunit, the photolabeled peptide CB9 was further cleaved by trypsin, and the tryptic digest was fractionated by gel filtration on a Bio-Gel P-4 column (Figure 5). In the elution profile, the radioactivity was entirely associated with the main peak of absorbancy corresponding to fractions 45–55. On the

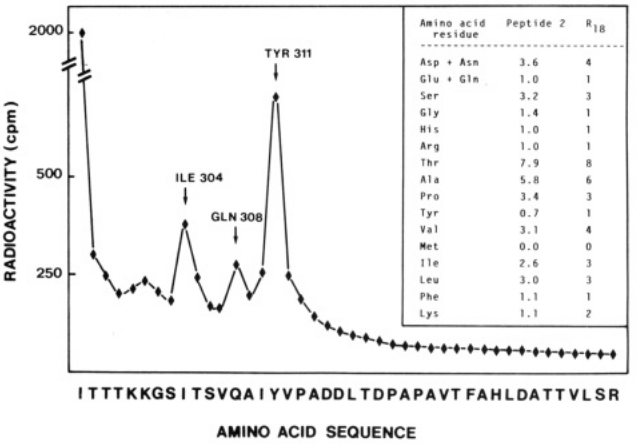

Amino acid residue	Peptide 2	R_{18}
Asp + Asn	3.6	4
Glu + Gln	1.0	1
Ser	3.2	3
Gly	1.4	1
His	1.0	1
Arg	1.0	1
Thr	7.9	8
Ala	5.8	6
Pro	3.4	3
Tyr	0.7	1
Val	3.1	4
Met	0.0	0
Ile	2.6	3
Leu	3.0	3
Phe	1.1	1
Lys	1.1	2

FIGURE 6: Edman degradation of radiolabeled peptide R_{18}. The peptide was immobilized on DITC glass beads and degraded in a solid-phase sequencer as described under Materials and Methods. The letters on the abscissa correspond to the amino acid sequence of the peptide. The released radioactivity at each cycle of the Edman degradation (not corrected for loss) showed two predominant labeled peaks at steps 9 and 16 corresponding to Ile 304 and Tyr 311 and one minor labeled peak at step 13 corresponding to Gln 308. In the insert, the amino acid compositions of peptides 2 and R_{18} are shown.

basis of its amino acid composition (insert of Figure 6) and the N-terminal amino acid residue, the material of this peak, called peptide 2, was identified as peptide R18 spanning Ile 296–Arg 337.

An aliquot of the R18 peptide was further subjected to cleavage by α-chymotrypsin, and the cleavage products were separated by reverse-phase HPLC on a C_8 Aquapore column (Brownlee). In the elution profile, the radioactivity was located in a single peak (not shown). The corresponding peptide had the same amino acid composition as that of the chymotryptic peptide, R18c, spanning Thr 299–Phe 326.

Identification of the Photolabeled Amino Acids in Peptide R18. After conversion of its C-terminal arginyl residue to ornithine, peptide R18 was attached to DITC glass beads and subjected to Edman degradation (Figure 6). Apart from the radioactivity measured at step 1, which was most probably due to the release of noncovalently bound peptide, radioactivity was predominantly released at steps 9 and 16, corresponding to Ile 304 and Tyr 311, and in lower amounts at step 13 corresponding to Gln 308. The labeling of Ile 304, Gln 308, and Tyr 311 was entirely consistent with the localization of radioactivity in the chymotryptic segment R18c extending from Thr 299 to Phe 326.

Discussion

Catalytic Sites and Noncatalytic Sites of Mitochondrial F_1: ANPP as a Probe of Catalytic Site. Beef heart F_1 contains a total of six adenine nucleotide binding sites. Photoactivatable nucleotide analogues have been extensively used to localize ADP and ATP binding sites on subunits of F_1. Depending on the type of F_1 investigated, i.e., mitochondrial, bacterial, or chloroplast F_1, on the experimental conditions, and on the nature of the photoactivatable nucleotide analogue utilized, F_1 nucleotide binding sites have been localized either on the α subunits, on the β subunits, or at the α/β interfaces [for review, see Vignais and Lunardi (1985)]. The possibility that this heterogeneous distribution was due to the photolabeling of catalytic and/or noncatalytic sites has to be considered. In this context it was of interest to explore the localization of the P_i binding site. Mitochondrial F_1 exhibits essentially one P_i binding site of relatively high affinity (K_d = 80 μM) (Penefsky, 1977). That this site is part of the F_1 catalytic site is based

on the following lines of evidence: (1) Inhibition of F_1-ATPase upon binding of the natural ATPase inhibitor is concomitant with the inhibition of P_i binding to F_1 (Klein et al., 1981), (2) P_i is rapidly released from F_1 by low concentrations of nucleotides, which results in the filling of the catalytic sites only by nucleotides (Beharry & Gresser, 1987), and (3) the fact that P_i can be condensed with ADP to form F_1-bound ATP in the presence of DMSO (Sakamoto & Tonomura, 1983) clearly indicates that the P_i binding site has a catalytic potentiality.

The P_i binding site of mitochondrial F_1 was located in the β subunit by means of an originally synthesized photoactivatable analogue of P_i, the 4-azido-2-nitrophenyl phosphate (ANPP) (Lauquin et al., 1980). This P_i analogue also binds to bacterial F_1 (Pougeois et al., 1983a) and chloroplast F_1 (Pougeois et al., 1983b). That ANPP binds to the same site as P_i was established from the following results: (1) P_i binding and ANPP binding to mitochondrial F_1 are mutually exclusive (Lauquin et al., 1980), (2) P_i is more effective than ADP and ATP for protection of CF_1 against photoinactivation by ANPP (Pougeois et al., 1983b), (3) ANPP promotes the quenching of the fluorescence of F_1–aurovertin as P_i does, whereas ADP stimulates the fluorescence level (cf. Results), and (4) ANPP inhibits competitively P_i transport by the mitochondrial P_i carrier. Furthermore, P_i and arsenate both protect the P_i carrier against photoinactivation by ANPP, whereas ADP does not (Tommasino et al., 1987).

Taken together, these results indicate that ANPP is a true P_i analogue and thus a potential probe for photolabeling of the P_i binding site of the catalytic site of F_1. In our experiments, only one labeled sequence was detected; thus there was no evidence for photolabeling of another P_i binding site which could be of low affinity (Kasahara & Penefsky, 1978).

Topographical Relationships between the Amino Acid Sequences Photolabeled by ANPP, 2-Azido-ADP, and 8-Azido-ATP: A Tentative Model for the Catalytic Site of Mitochondrial F_1. In the present work, the use of [^{32}P]ANPP, an analogue of P_i, has made it possible to delineate in beef heart F_1 a peptide sequence that specifically interacts with the photoreactive group of the photoprobe and is therefore presumed to be in the close neighborhood of the P_i site. This sequence is located in the β subunit; it spans residues Ile 304–Tyr 311.

In a previous paper (Garin et al., 1986), we reported that upon photoirradiation of native beef heart F_1 in the presence of 2-azido-ADP or 2-azido-ATP, four amino acids of the β subunit belonging to the rapidly exchangeable nucleotide binding sites were photolabeled, namely, Leu 342, Ile 344, Tyr 345, and Pro 346. Interestingly, Tyr 345 is specifically labeled by [^{3}H]-5′-[*p*-(fluorosulfonyl)benzoyl]inosine (FSBI), an affinity analogue of ITP (Bullough & Allison, 1986). FSBI is expected to bind only to the catalytic site of F_1, as ITP does (Schuster et al., 1975), which brings additional evidence that Tyr 345 is at the catalytic site.

2-Azido-ADP can fill the six vacant nucleotide binding sites of nucleotide-depleted mitochondrial F_1 (Lunardi et al., 1987). When photolabeling was performed under these conditions, it was found that 2-azido-ADP bound not only to the Tyr 345 region of the β subunit but also to a sequence of this subunit that extends from Gly 72 to Arg 83 (Lunardi et al., 1987). From these results it was concluded that, in the β subunit of mitochondrial F_1, the Leu 342–Pro 346 and Gly 72–Arg 83 sequences interact with the azido group of 2-azido-ADP bound at catalytic sites and noncatalytic sites, respectively (Lunardi et al., 1987). Another sequence belonging to noncatalytic sites and containing Tyr 368 was recently found in the β subunit of mitochondrial F_1 (Cross et al., 1987).

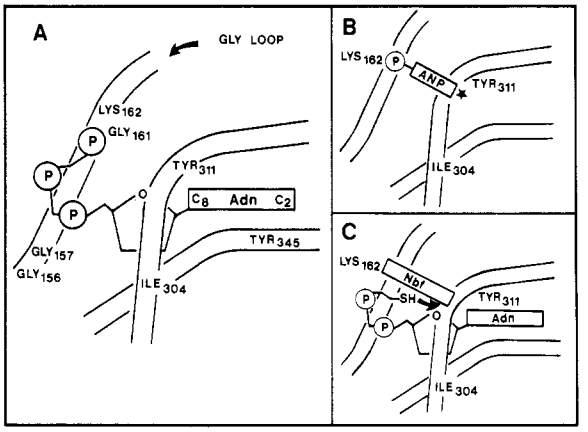

FIGURE 7: A possible model for the catalytic site of mitochondrial F_1-ATPase. (A) Insertion of the adenine ring of ATP in a crevice with interactions of carbon 2 with the Tyr 345 region and carbon 8 with the Tyr 311 region. The phosphate chain interacts with a glycine-rich portion of the β chain (Gly loop). (B) Interaction between the azido group (illustrated by a star) of ANPP and the Tyr 311 region on one hand and the interaction between the phosphate group of ANPP and the Gly loop on the other. (C) Diagram showing how AMEDA removes Nbf from Tyr 311 (Wu et al., 1987).

8-Azido-ATP was reported to photolabel a sequence of amino acids in the β subunit of beef heart F_1, including Lys 301, Ile 304, and Tyr 311 (Hollemans et al., 1983), located at a distance from that photolabeled by 2-azido-ADP or 2-azido-ATP. These photolabeling experiments were tentatively interpreted (Garin et al., 1986) on the basis that the adenine ring of ADP or ATP bound to the catalytic site of mitochondrial F_1 was buried in a crevice. Carbons 2 and 8, which are located on opposite faces of the adenine ring, were suggested to interact with the edges of a crevice containing the sequences Lys 301–Tyr 311 and Leu 342–Pro 346, respectively. This hypothesis was based on the postulate that 2-azido and 8-azido nucleotides bind to F_1 in the same conformation, in spite of the fact that free 8-azido nucleotides are predominantly in the syn conformation (Sarma et al., 1974) and 2-azido nucleotides in the anti conformation (Czarnecki, 1984). This postulate has been recently verified (Garin and Gronenborn, unpublished results) by H NMR experiments, using transferred nuclear Overhauser enhancement (TRNOE). The results showed that 8-azido nucleotides are bound to the exchangeable sites of F_1 in the anti conformation as ATP, ADP, and 2-azido nucleotides are.

The fact that virtually the same amino acid sequence is photolabeled by 8-azido-ATP and ANPP suggests the possibility that, in the catalytic site of F_1, P_i lies close to the carbon 8 of adenine (Figure 7A,B). It is presumed that, for steric reasons inherent in the condensation of P_i and ADP to form ATP at the catalytic site of F_1, P_i and the γ-phosphate of ATP occupy positions not too distant from each other (Figure 7A). It must be added that the proximity of the phosphate chain and the carbon 8 of ATP (or ADP), which is deduced from photolabeling experiments, is consistent with molecular models which show that in the anti conformation the phosphate chain of ADP or ATP is much closer to carbon 8 than to carbon 2 of adenine.

In the context of the interactions between P_i, ADP, and ATP binding sites of mitochondrial F_1, it is worth discussing some binding data concerning nitrobenzofurazan (Nbf), an inhibitor of F_1-ATPase, which binds to β-Tyr 311 at neutral pH (Andrews et al., 1984a; Sutton & Ferguson, 1985) as [^{32}P]ANPP does. The mechanism of inactivation of F_1 by Nbf has been

a matter of debate. Some confusion stemmed from the finding that binding of Nbf to F_1 in reconstituted submitochondrial particles affects ATP hydrolysis much more than it does ATP synthesis (Steimeier & Wang, 1979; Kohlbrenner & Boyer, 1982), leading to the hypothesis that Nbf might bind to a regulatory site. However, as in this reconstituted system the coupling of ATP synthesis to the proton gradient was possibly a rate-limiting step, no definite conclusion appeared to be warranted. This debate has been recently clarified by the work of Perez et al. (1986), showing that inhibition of mitochondrial and bacterial membrane-bound F_1 and isolated F_1 by Nbf is strongly protected by binding of P_i to the catalytic site. Perez et al. (1986) concluded that a role for β-Tyr 311 in mitochondrial F_1 at or near the catalytic site warrants serious consideration. In addition, it was recently reported (Wu et al., 1987) that inhibition of mitochondrial F_1-ATPase by the reversible binding of Nbf to β-Tyr 311 of mitochondrial F_1 is relieved upon addition of P^1-(5′-adenosyl) P^2-N-(2-mercaptoethyl)diphosphoramidate (AMEDA), an analogue of ATP terminated by a thiol group. The explanation favored by the authors was that AMEDA reacts by its terminal thiol with Nbf bound to Tyr 311, to form an AMEDA–Nbf complex. This is accompanied by the release of Nbf from Tyr 311 and the recovery of ATPase activity. This result and the structural similarity between AMEDA and ATP were regarded by Wu et al. (1987) as compelling evidence for the presence of Nbf-labeled Tyr 311 near the γ-phosphate group of ATP bound at the catalytic site of F_1 (Figure 7C). All these data taken together support the contention that P_i and the γ-phosphate group of ATP bind at the catalytic site close to Tyr 311.

By shifting the pH to alkaline values, Nbf is transferred from Tyr 311 to a lysine residue of the β subunit (Ferguson et al., 1975) which has been identified as Lys 162 (Andrews et al., 1984b). For transfer to occur, it is clear that Tyr 311 and Lys 162 must be close to each other, which requires a specific folding of the β chain. As previously discussed (Garin et al., 1986; Duncan et al., 1986), Lys 162 belongs to a glycine-rich sequence ("Gly loop") of the β subunit. A similar glycine-rich sequence has been reported to occur in a number of nucleotide binding proteins and to be in contact with the phosphate chain of the bound nucleotides (Walker et al., 1982; Möller & Amons, 1985; Mc Cormick et al., 1985; Fry et al., 1986). Consistent with the postulated function of the Gly loop, mutations within this conserved sequence of the β subunit of *E. coli* F_1 result in catalytic defects (Hsu et al., 1987; Parsonage et al., 1987). [^{32}P]ANPP, which photolabels the Tyr 311 region of the β subunit of mitochondrial F_1 by its azido group, might interact with the Gly loop of the same subunit by its phosphate group which is 4 Å distant from the azido group, as illustrated in the scheme of Figure 7B.

Acknowledgments

We thank Jeannine Bournet for typing the manuscript.

Registry No. ATPase, 9000-83-3; ANPP, 74784-75-1; P_i, 14265-44-2.

References

Amory, A., Foury, F., & Goffeau, A. (1980) *J. Biol. Chem. 255*, 9353–9357.

Anderson, F. S., & Murphy, R. C. (1976) *J. Chromatogr. 121*, 151–262.

Andrews, W. W., Hill, F. C., & Allison, W. S. (1984a) *J. Biol. Chem. 259*, 8219–8225.

Andrews, W. W., Hill, F. C., & Allison, W. S. (1984b) *J. Biol. Chem. 259*, 14378–14382.

Beharry, S. B., & Gresser, M. J. (1987) *J. Biol. Chem. 262*, 10630–10637.

Birdsall, B., King, R. W., Wheeler, M. R., Lewis, C. A., Goode, S. R., Dunlap, R. B., & Roberts, G. C. K. (1983) *Anal. Biochem. 132*, 353–361.

Bradford, M. M. (1976) *Anal. Biochem. 72*, 248–254.

Bullough, D. A., & Allison, W. S. (1986) *J. Biol. Chem. 261*, 14171–14177.

Chang, J. Y. (1979) *Biochim. Biophys. Acta 578*, 188–195.

Crivellone, M. D., Hermodson, M., & Axelrod, B. (1985) *J. Biol. Chem. 260*, 2657–2661.

Cross, R. L., Cunningham, D., Miller, C. G., Xue, Z., Zhou, J., & Boyer, P. (1987) *Proc. Natl. Acad. Sci. U.S.A. 84*, 5715–5719.

Czarnecki, J. J. (1984) *Biochim. Biophys. Acta 300*, 41–51.

Duncan, T. M., Parsonage, D., & Senior, A. E. (1986) *FEBS Lett. 208*, 1–6.

Ferguson, S. J., Lloyd, W. J., Lyons, M. H., & Radda, G. K. (1975) *Eur. J. Biochem. 54*, 117–126.

Fry, D. C., Kuby, S. A., & Mildvan, A. S. (1985) *Proc. Natl. Acad. Sci. U.S.A. 83*, 907–911.

Garin, J., Boulay, F., Issartel, J. P., Lunardi, J., & Vignais, P. V. (1986) *Biochemistry 25*, 4431–4437.

Hartwick, R., Jeffries, A., Krstulovic, A., & Brown, P. R. (1978) *J. Chromatogr. Sci. 16*, 427–435.

Hollemans, M., Runswick, M. J., Fearnley, I. M., & Walker, J. E. (1983) *J. Biol. Chem. 258*, 9307–9313.

Hoppe, J., Gatti, D., Weber, H., & Sebald, W. (1986) *Eur. J. Biochem. 155*, 259–264.

Hsu, S., Noumi, T., Takeyama, M., Maeda, M., Ishibashi, S., & Futai, M. (1987) *FEBS Lett. 218*, 222–226.

Issartel, J. P., Klein, G., Satre, M., & Vignais, P. V. (1983) *Biochemistry 22*, 3492–3497.

Kasahara, M., & Penefsky, H. S. (1978) *J. Biol. Chem. 253*, 4180–4187.

Klein, G., Lunardi, J., & Vignais, P. V. (1981) *Biochim. Biophys. Acta 636*, 185–192.

Klein, G., Satre, M., Zaccaï, G., & Vignais, P. V. (1982) *Biochim. Biophys. Acta 681*, 226–236.

Knowles, A. F., & Penefsky, H. S. (1972) *J. Biol. Chem. 247*, 6617–6623.

Kohlbrenner, W. E., & Boyer, P. D. (1982) *J. Biol. Chem. 257*, 3441–3446.

Lauquin, G., Pougeois, R., & Vignais, P. V. (1980) *Biochemistry 19*, 4620–4626.

Lee, Y. M., & Benisek, W. F. (1978) *J. Biol. Chem. 253*, 5460–5463.

Lunardi, J., Garin, J., Issartel, J. P., & Vignais, P. V. (1987) *J. Biol. Chem. 262*, 15172–15181.

Mac Keag, M., & Brown, P. R. (1978) *J. Chromatogr. 152*, 253–254.

Mc Cormick, F., Clarck, B. F. C., La Cour, T. F. M., Kjeldgaard, M., Norskov-Lauritsen, L., & Nyborg, J. (1985) *Science (Washington, D.C.) 230*, 78–82.

Möller, W., & Amons, R. (1985) *FEBS Lett. 186*, 1–7.

Morris, H. R., Dickinson, R. J., & Williams, D. H. (1973) *Biochem. Biophys. Res. Commun. 51*, 247–255.

Parsonage, D., Wilke-Mounts, S., & Senior, A. E. (1987) *J. Biol. Chem. 262*, 8022–8026.

Patterson, H. S., & Greene, R. C. (1965) *Anal. Chem. 37*, 854–857.

Penefsky, H. S. (1977) *J. Biol. Chem. 252*, 2891–2899.

Perez, J. A., Greenfield, A. J., Sutton, R., & Ferguson, R. J. (1986) *FEBS Lett. 198*, 113–118.

Pougeois, R., Lauquin, G., & Vignais, P. V. (1983a) *FEBS Lett. 153*, 65–70.
Pougeois, R., Lauquin, G., & Vignais, P. V. (1983b) *Biochemistry 22*, 1241–1245.
Runswick, M. J., & Walker, J. E. (1983) *J. Biol. Chem. 258*, 3081–3089.
Sakamoto, J., & Tonomura, Y. (1983) *J. Biochem. 93*, 1601–1614.
Sarma, R. H., Lee, C. H., Evans, F. E., Yathindra, N., & Sundaralingam, M. (1974) *J. Am. Chem. Soc. 96*, 7337–7348.
Schuster, S. M., Ebel, R. E., & Lardy, H. A. (1975) *J. Biol. Chem. 250*, 7848–7853.
Smith, A. L. (1967) *Methods Enzymol. 10*, 81–86.
Steczko, J., Hermodson, M., Axelrod, B., & Dziembor-Kentzer, E. (1983) *J. Biol. Chem. 258*, 13148–13154.
Steinmeier, R. C., & Wang, J. H. (1979) *Biochemistry 18*, 111–118.
Sutton, R., & Ferguson, S. J. (1985) *Eur. J. Biochem. 148*, 551–554.
Symons, R. H. (1968) *Biochim. Biophys. Acta 155*, 609–610.
Tomaszek, T. A., & Schuster, S. M. (1986) *J. Biol. Chem. 261*, 2264–2269.
Tommasino, M., Prezioso, G., & Palmieri, F. (1987) *Biochim. Biophys. Acta 890*, 39–46.
Vignais, P. V., & Lunardi, J. (1985) *Annu. Rev. Biochem. 54*, 977–1014.
Walker, J. E., Saraste, M., Runswick, M. J., & Gay, N. J. (1982) *EMBO J. 1*, 945–951.
Wu, J. C., Chuan, H., & Wang, J. H. (1987) *J. Biol. Chem. 262*, 5145–5150.

Redox Cofactor Interactions in Photosystem II: Electron Spin Resonance Spectrum of P_{680}^+ Is Broadened in the Presence of Y_Z^+†

Curtis W. Hoganson‡ and Gerald T. Babcock*
Department of Chemistry, Michigan State University, East Lansing, Michigan 48824
Received June 27, 1988; Revised Manuscript Received October 18, 1988

ABSTRACT: The electron spin resonance spectrum of P_{680}^+ has been measured in photosystem II membranes at room temperature under repetitive flash excitation by using gated integration techniques. Oxygen evolution was inhibited in the samples used in these experiments, and the lifetime of the radical is extended into the 150–200-μs range. Three different treatments were used that allowed us to determine the spectral characteristics of P_{680}^+ when the paramagnetic species Y_Z^+ was also present. These results were compared to the P_{680}^+ spectral properties that we measured under conditions in which Y_Z was in its reduced, diamagnetic form. With Tris-inactivated membranes, where Y_Z^+ but not manganese was present, only a low P_{680}^+ signal amplitude could be measured, which precluded an accurate determination of the line width. With NaCl-washed membranes and membranes treated with $K_3Fe(CN)_6$, in which Y_Z^+ and manganese were both present during the measurement, the field-modulated P_{680}^+ spectrum is 8.9 G wide. This is 1 G wider than the spectrum measured when Y_Z remains reduced, as happens in membranes inhibited with NH_2OH. The broadening of the P_{680}^+ spectrum that occurs when its immediate donor is oxidized is attributed to a magnetic dipole–dipole interaction between P_{680}^+ and Y_Z^+. The extent of broadening allows us to estimate that the center-to-center distance between the two radicals is 10–15 Å.

Photosystem II uses light energy to create a chlorophyll cation radical, P_{680}^+,[1] which is a strong oxidant. A cluster of four manganese atoms in the oxygen-evolving complex (OEC) stores the equivalents generated by four consecutive photooxidations of P_{680} and catalyzes the oxidation of water. To convey oxidizing equivalents from P_{680}^+ to the manganese, a tyrosine residue (Barry & Babcock, 1987; Hoganson & Babcock, 1988; Gerken et al., 1988), called Y_Z, undergoes reversible one-electron oxidation to form a radical with a characteristic ESR line shape (signal II). Normally, these reactions are fast: the electron transfer from Y_Z to P_{680}^+ occurs in 20–250 ns; the electron transfer from the OEC to Y_Z^+ occurs in 30–1300 μs. Certain chemical treatments inhibit oxygen evolution and can greatly retard or entirely abolish these electron transfers, thereby lengthening the lifetime of the radicals and facilitating spectroscopic examination of them [for a review, see Babcock (1987)].

P_{680} and Y_Z are located in the reaction center of PSII, composed of the 32- and 34-kDa polypeptides, D1 and D2, respectively, and the 9- and 4-kDa polypeptides of cytochrome *b*-559 (Nanba & Satoh, 1987). P_{680} is probably bound to both D1 and D2 (Michel & Deisenhofer, 1986, 1988), and Y_Z is likely to be a residue of the D1 polypeptide (Debus et al., 1988a,b). Although detailed folding models for D1 and D2 are available (Trebst, 1986) and have received experimental support (Sayre et al., 1987), the spatial arrangement of the electron transfer components within the reaction center remains obscure.

† This research was supported by the U.S. Department of Agriculture, Competitive Research Grants Office, Photosynthesis Program, and by the McKnight Foundation.
‡ Present address: Department of Biochemistry and Biophysics, Chalmers Institute of Technology, S-412 96 Goteborg, Sweden.

[1] Abbreviations: DCMU, 3-(3,4-dichlorophenyl)-1,1-dimethylurea; ESR, electron spin resonance; OEC, oxygen-evolving complex; P_{680}, primary donor of PSII; PSII, photosystem II; Q_A, electron acceptor of PSII; Tris, tris(hydroxymethyl)aminomethane; Y_D^+, stable tyrosine radical in PSII; Y_Z, electron donor to P_{680}^+, also a tyrosine.

0006-2960/89/0428-1448$01.50/0 © 1989 American Chemical Society